



# Copper Immobilization on $\text{Fe}_3\text{O}_4$ @Agar: An Efficient Superparamagnetic Nanocatalyst for Green Ullmann-Type Cross-Coupling Reaction of Primary and Secondary Amines with Aryl Iodide Derivatives

Kimia Hoseinzade<sup>1</sup> · Seyed Ali Mousavi-Mashhadi<sup>1</sup> · Ali Shiri<sup>1</sup>

Received: 24 May 2021 / Accepted: 11 September 2021

© The Author(s), under exclusive licence to Springer Science+Business Media, LLC, part of Springer Nature 2021

## Abstract

Immobilization of copper on magnetic nanoparticles was performed using surface rectification of  $\text{Fe}_3\text{O}_4$  with Agar. The magnetic  $\text{Fe}_3\text{O}_4$ @Agar–Cu nanocatalyst was prepared and entirely characterized by different analyses such as Fourier transform infrared, X-ray diffraction, scanning electron microscopy, transmission electron microscopy, vibrating sample magnetometry, energy dispersive X-ray, thermogravimetric, and inductively coupled plasma. The nanocatalyst was applied to C–N bond forming Ullmann-type Cross-Coupling reaction between aryl halides and primary or secondary amines using water as a green medium. The results of the Ullmann Cross-Coupling reaction by  $\text{Fe}_3\text{O}_4$ @Agar–Cu magnetic nanoparticles as catalyst demonstrate excellent activity and stability in water. Moreover, this catalyst can be recycled several times without considerable loss in its activity.

**Keywords** Agar · Ullmann-type Cross-Coupling reaction · C–N cross-coupling · Green chemistry · Nano  $\text{Fe}_3\text{O}_4$  · Water

## 1 Introduction

In recent decades, the lack of green processes in the chemical fields and industries is a significant concern. Green Chemistry is effective for human health and necessary to protect the environment [1–5]. Concern of pollutions, toxicity, and waste treatment methods are an essential issue for all chemists to use neat solvents, especially water, in their chemical processes because of the availability, recyclability, thermal stability and chemical conditions [6–11].

There is lots of investigation to find a better catalyst, ligand, base, or more effective solvents for C–N cross-coupling reactions. Considering an influential catalyst that can be utilized for both primary and secondary amines and act as a regioselective catalysts in satisfying yields have been investigated extensively [12–16]. The Buchwald–Hartwig is an essential reaction since aryl amines are commonly used in pharmaceutical treatments, materials, and drugs

with interesting electronic properties [17]. *Neratinib* was approved in 2017 for the treatment of positive breast cancer (Fig. 1I). *Abemaciclib* as a cyclin-dependent kinase inhibitor, is used for the treatment of breast cancer.  $\text{Pd}_2(\text{dba})_3$  can catalyze the Buchwald–Hartwig reaction using Xantphos as a ligand to achieve the *Abemaciclib* drug (Fig. 1II) [18].

Recently, the use of catalysts in many forms is a primary topic in organic chemistry [19–21]. Especially, using magnetite as one of the best support surfaces is guaranteed some properties such as the control of unwanted reactions, the stability of pH, the simplicity of the separation method and reusing of the catalyst several times, high surface area and low toxicity [22–28].

The first catalyst that represented for Buchwald–Hartwig reaction was the Pd metal complex by organic or inorganic ligands that were accepted as the best catalyst in recent years [29–32]. Buchwald et al. reported efficient catalysts for the catalytic amination of a wide variety of aryl halides and triflates in 2000 [33]. The palladium-catalyzed amination of aryl halides had been successfully known as an important method for the Buchwald–Hartwig C–N cross-coupling reaction. A variety of catalysts represented for this reaction such as  $(\text{Fe}_3\text{O}_4$ @

✉ Ali Shiri  
alishiri@um.ac.ir

<sup>1</sup> Department of Chemistry, Faculty of Science, Ferdowsi University of Mashhad, Mashhad, Iran

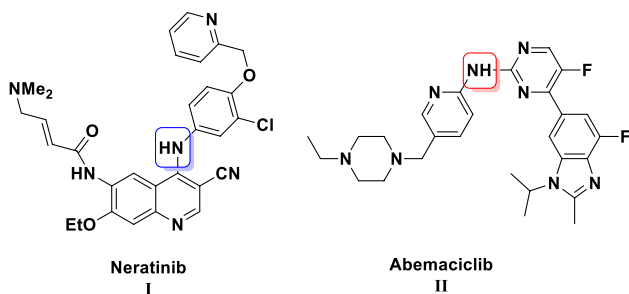
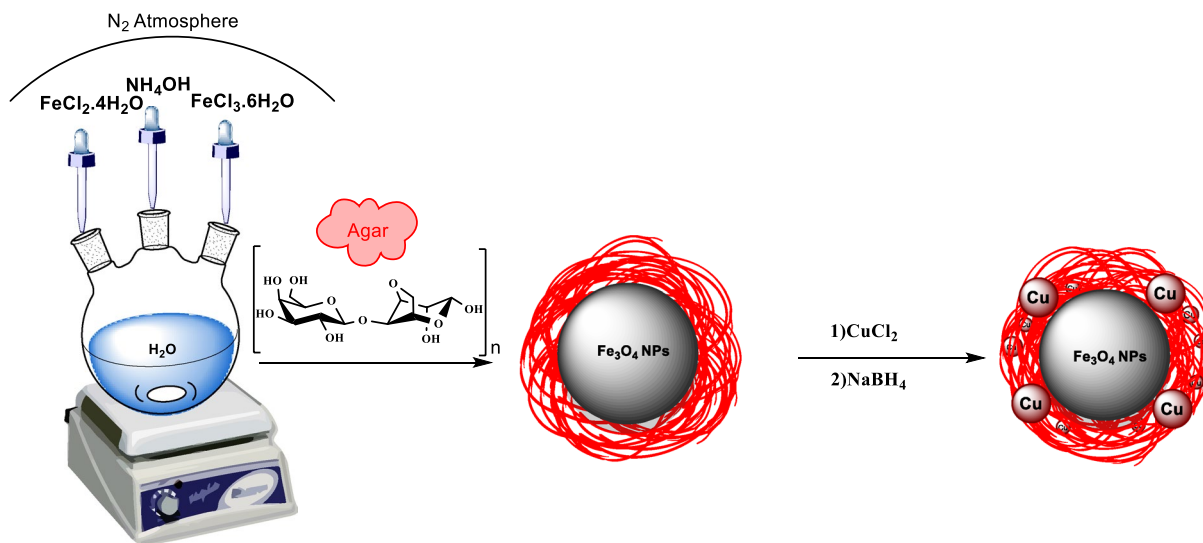


**Fig. 1** Examples of C–N cross-coupling reaction in dugs treatment

PDA/Pd(II) [34], (Zn(OAc)<sub>2</sub>) [35], (NiCl(bpy)(IPr)) [36]. There are still limitations in some processes affiliated with transition metal, specifically using Pd [37–43], for example, using these high-cost metals and the difficult process in the workup [44]. In the study of the reaction, Cu is one

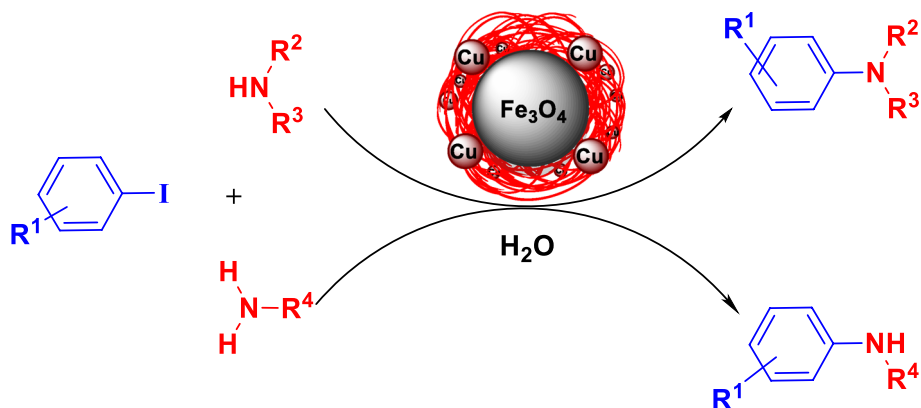
of the most incredible noble element that can be considered for the Ullmann type reaction with a solid support Cu-catalyst as an alternative to Pd catalyzed cross-couplings. Agar as a plentiful, non-toxic, cheap, and natural biopolymer, is considered as a linker for this kind of catalyst [45–52]. It can be found in the cell wall of some red algae and its strong gelling seaweed hydrocolloid composed [53]. Hitherto, the main structure of Agar–Agar is chemically characterized by the repeating units of D-galactose and 3,6-anhydro-L-galactose. Also, it has a chiral surface with free hydroxyl groups that could act as hydrogen bond donors or acceptors [51, 54].

Based on the above information and our previous studies [31, 55–57], we present an effective nanocatalyst to perform the Ullmann Cross-Coupling reaction by considering Cu<sup>(0)</sup> as a new catalyst system with fascinating properties in comparison with palladium, agar as the linker, and magnetite as the support (Scheme 1 and 2).



**Scheme 1** Synthesis of Fe<sub>3</sub>O<sub>4</sub>@Agar–Cu NPs catalyst

**Scheme 2** General procedure for C–N bond cross-coupling reactions



## 2 Results and Discussion

### 2.1 The Preparation and Characterization of the Catalyst

The catalyst was prepared according to Scheme 1. The nano magnetite ( $\text{Fe}_3\text{O}_4$  NPs) was synthesized according to the literature [22]. The agar polysaccharide was immobilized around the prepared  $\text{Fe}_3\text{O}_4$  NPs. Then, copper was incorporated successfully among the agar linker at the same time. The catalyst structure was characterized using different analyses, including FT-IR, XRD, SEM, TEM, VSM, EDX, and TGA.

In Fig. 2, the FT-IR spectrum demonstrated the absorptions of Agar ( $1070\text{ cm}^{-1}$ ) appear along with a peak at  $582\text{ cm}^{-1}$  which corresponds to the stretching vibration band of the Fe–O group in  $\text{Fe}_3\text{O}_4$ @Agar. This indicates that magnetic  $\text{Fe}_3\text{O}_4$  NPs were coated by Agar. Possible bindings of copper with OH group in  $\text{Fe}_3\text{O}_4$ @Agar–Cu NPs have decreased the combined intensity of hydroxyl peaks at  $3356\text{ cm}^{-1}$ . Splitting of the bending bands of hydroxyl at  $1614\text{ cm}^{-1}$  and  $1352\text{ cm}^{-1}$  also indicate the bonding of Cu with OH moiety. The variations in the region of  $1350\text{ cm}^{-1}$  and  $1000\text{ cm}^{-1}$  can be attributed to the perturbation in C–O vibrations induced by Agar–Cu complexation (Fig. 2).

The XRD patterns help define the crystal structures of  $\text{Fe}_3\text{O}_4$ @Agar NPs and  $\text{Fe}_3\text{O}_4$ @Agar–Cu NPs. Sharp peaks vouch for the excellent crystallinity of the prepared

samples (Fig. 3). For  $\text{Fe}_3\text{O}_4$ @Agar NPs, the outcome is in agreement with the standard patterns of inverse cubic spinel magnetite ( $\text{Fe}_3\text{O}_4$ ) crystal structure, showing six diffraction peaks at  $2\theta$  about  $35.5^\circ$ ,  $43.3^\circ$ ,  $56.9^\circ$ ,  $62.6^\circ$ ,  $62.8^\circ$ , and  $74.1^\circ$  marked by their corresponding indices (3 1 1), (4 0 0), (3 3 3), (4 0 4), (4 0 4), and (5 3 3), respectively. The small and weak broad bands in the span of  $21^\circ$ – $28^\circ$  indicate the existence of Agar. Diffraction patterns of the  $\text{Fe}_3\text{O}_4$ @Agar–Cu NPs exhibit three additional peaks at  $2\theta$  about  $43.3^\circ$ ,  $50.2^\circ$ , and  $74.1^\circ$ ; corresponding to (1 1 1), (2 0 0), and (2 0 2) planes of face-centered cubic (fcc) copper crystal structure. No impurities in the XRD patterns infer the formation of net  $\text{Fe}_3\text{O}_4$  and Cu nanoparticles.

The morphological features were studied using the SEM technique. The SEM imaging of the nanoparticles are almost spherical, narrowly distributed, well dispersed, and with a core–shell structural form, and also shows nanometer-sized particles of the catalyst is less than 25 nm in diameter. However, it presumed that this particle size causes the catalyst to be more in touch with the reactants, which leads to a good yield of the desired product (Fig. 4).

TEM image of the catalyst has been shown in Fig. 5. The spherical shape of each nanoparticle corresponded to the core of the catalyst, similar to SEM image which can be observed at a scale of less than 25 nm. Also, TEM images show that magnetic nanoparticles of  $\text{Fe}_3\text{O}_4$  have been encapsulated by the biopolymeric network of Agar.

Magnetic hysteresis measurements of  $\text{Fe}_3\text{O}_4$ @Agar (Fig. 6a) and  $\text{Fe}_3\text{O}_4$ @Agar–Cu (Fig. 6b) NPs were created in the limited area – 15,000 to 15,000 Oe using VSM. As

**Fig. 2** FT-IR spectrum of **a**  $\text{Fe}_3\text{O}_4$ @Agar NPs and **b**  $\text{Fe}_3\text{O}_4$ @Agar–Cu NPs

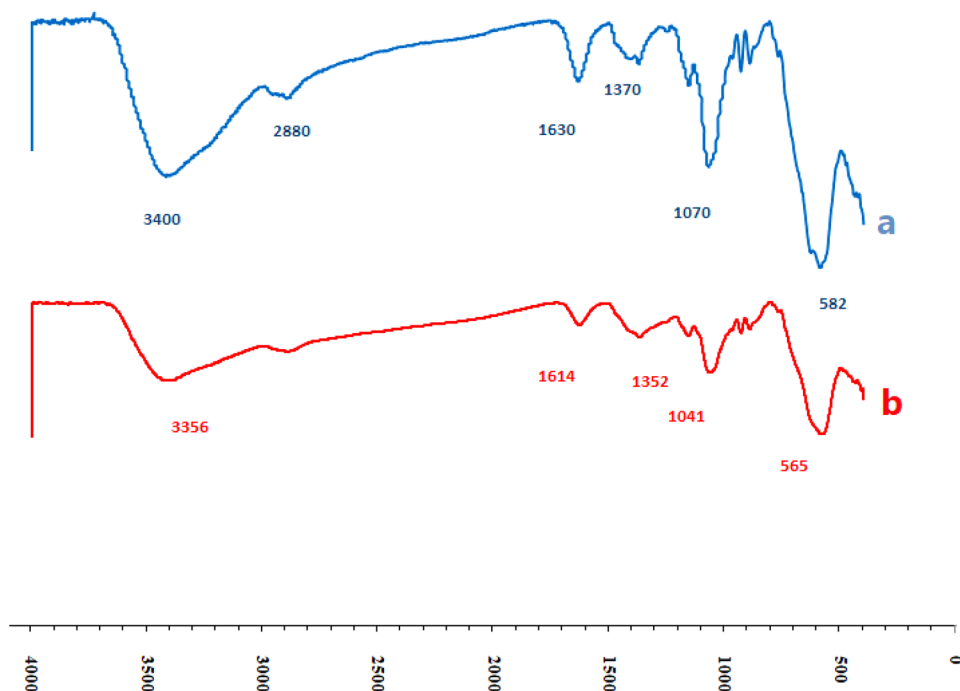


**Fig. 3** X-ray diffraction spectroscopy for  $\text{Fe}_3\text{O}_4$ @Agar-Cu NPs

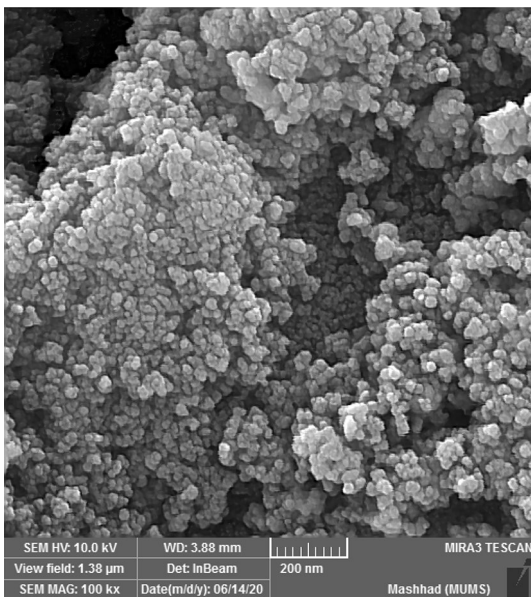
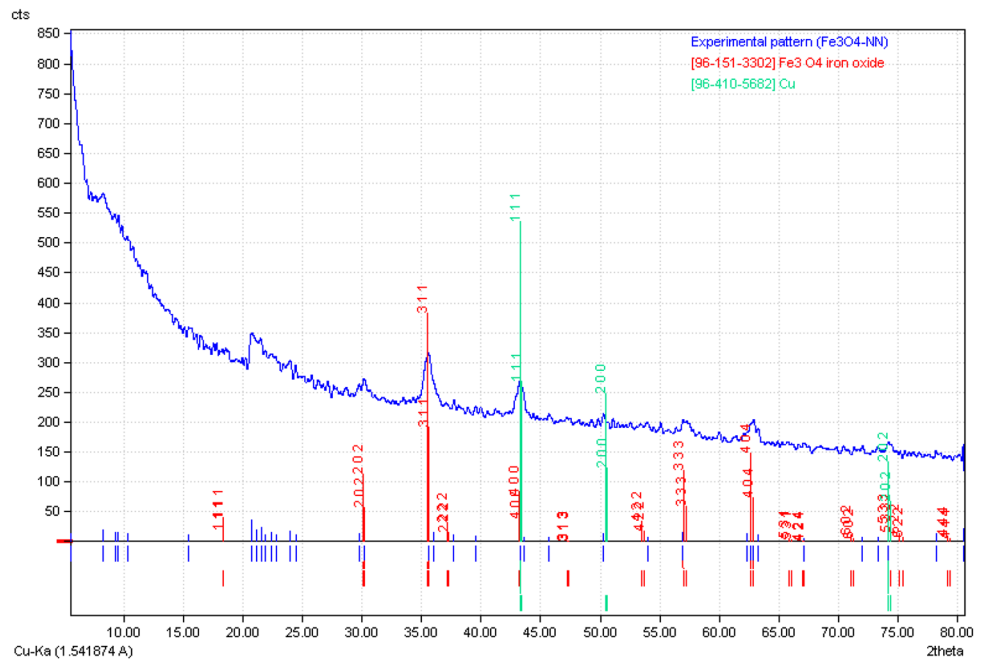


**Fig. 4** Scanning electron microscopy (SEM) for  $\text{Fe}_3\text{O}_4$ @Agar-Cu NPs at 200 nm

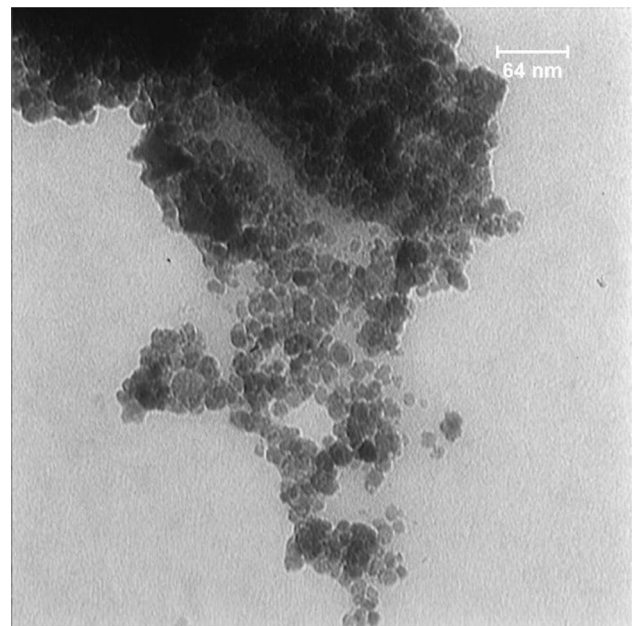


**Fig. 5** Transmission electron microscopy (TEM) for  $\text{Fe}_3\text{O}_4$ @Agar-Cu NPs at 64 nm

shown in Fig. 6, the saturation magnetization of  $\text{Fe}_3\text{O}_4$ @Agar-Cu NPs is about  $35 \text{ emu g}^{-1}$ , lower than that of  $\text{Fe}_3\text{O}_4$ @Agar ( $33 \text{ emu g}^{-1}$ ). The magnetization curve displays that the  $\text{Fe}_3\text{O}_4$ @Agar-Cu NPs have paramagnetic attributes in which the nanoparticles can be easily separated from the reaction melange using an external magnet.

To specify the elemental composition of  $\text{Fe}_3\text{O}_4$ @Agar-Cu NPs, EDX analysis was fulfilled (Fig. 7). The EDX

pattern supports excellent dispersion of  $\text{Fe}_3\text{O}_4$ @Agar-Cu NPs. Chemical characterization of the nanoparticles showed that they were composed of iron, carbon, oxygen, and copper elements, and this analysis detect the presence of 7.21 mol% Cu in  $\text{Fe}_3\text{O}_4$ @Agar-Cu NPs.

TGA of  $\text{Fe}_3\text{O}_4$ @Agar-Cu NPs was manipulated in the range of 20–550 °C (Fig. 8). The first mass loss of  $\text{Fe}_3\text{O}_4$ @Agar-Cu NPs at below 190 °C is due to the removal of

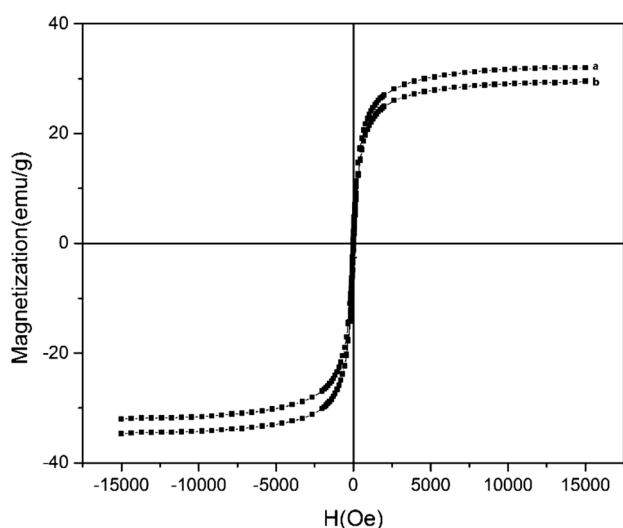


**Fig. 6** Vibrating-sample magnetometer (VSM) spectroscopy **a**  $\text{Fe}_3\text{O}_4$ @Agar and **b**  $\text{Fe}_3\text{O}_4$ @Agar-Cu NPs

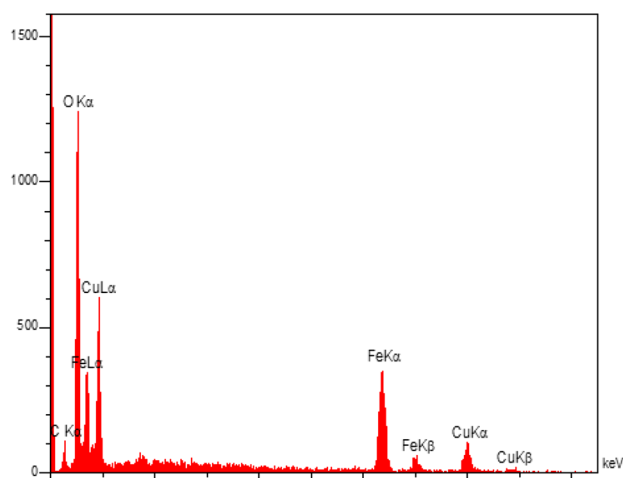


**Fig. 7** Energy-dispersive X-ray spectroscopy for  $\text{Fe}_3\text{O}_4$ @Agar-Cu NPs

physically adsorbed water. The second and the major weight loss ( $-40.16\%$ ) of  $\text{Fe}_3\text{O}_4$ @Agar-Cu NPs in the range of  $200\text{ }^\circ\text{C}$  to  $380\text{ }^\circ\text{C}$  is ascribed to Agar as the organic moiety. It is concluded that the most of the weight of the catalyst is related to  $\text{Fe}_3\text{O}_4$  as the mineral part.

## 2.2 Catalytic Application of $\text{Fe}_3\text{O}_4$ @Agar-Cu Catalyst

After the characterization of the catalyst structure, the newly prepared catalyst efficiency has been investigated in the Ullmann Cross-Coupling reaction. Initially, in order to optimize the model reaction conditions of iodobenzene with aniline, some parameters, including solvents, amounts of catalyst,

temperature and the time of reaction were scrutinized thoroughly (Table 1). The impact of the catalyst was inspected with different amounts of  $\text{Fe}_3\text{O}_4$ @Agar-Cu. The reaction did not proceed in the absence of the catalyst even after 15 h. The effect of solvents was also examined by polar and non-polar solvents, including DMSO, DMF, Toluene and water. Fortunately, a high yield was observed in  $\text{H}_2\text{O}$  as a green and sustainable solvent. The effect of time duration and temperature on the model reaction was also evaluated, and it was found the best time and temperature are considered as 12 h in  $100\text{ }^\circ\text{C}$  with excellent yield.

Next, in order to expand the scope of this reaction, various derivatives of C-N bond cross-coupling reactions have been represented in Table 2. This catalyst can be used for both primary and secondary arylamines with proper yields, which rarely reported formerly. There are not any significant differences in reaction yields considering various amines (primary or secondary) bearing electron-donating or electron-withdrawing groups, and all related products were obtained in good to excellent yields. Also, for improving the validity of the synthesis field and larger scale of the reaction, 2-amino-3-cyano-7,7-dimethyl-5-oxo-4-phenyl-5,6,7,8-tetrahydro-4H-chromene (entry 16) was considered as complicated amine structure. It was conducted in Ullmann Cross-Coupling amination reaction using  $\text{Fe}_3\text{O}_4$ @Agar-Cu NPs as the catalyst. The result showed the complete performance of the reaction and remarkable yield based on confirmation by mass spectroscopy,  $^1\text{H}$ , and  $^{13}\text{C}$  NMR analyses.

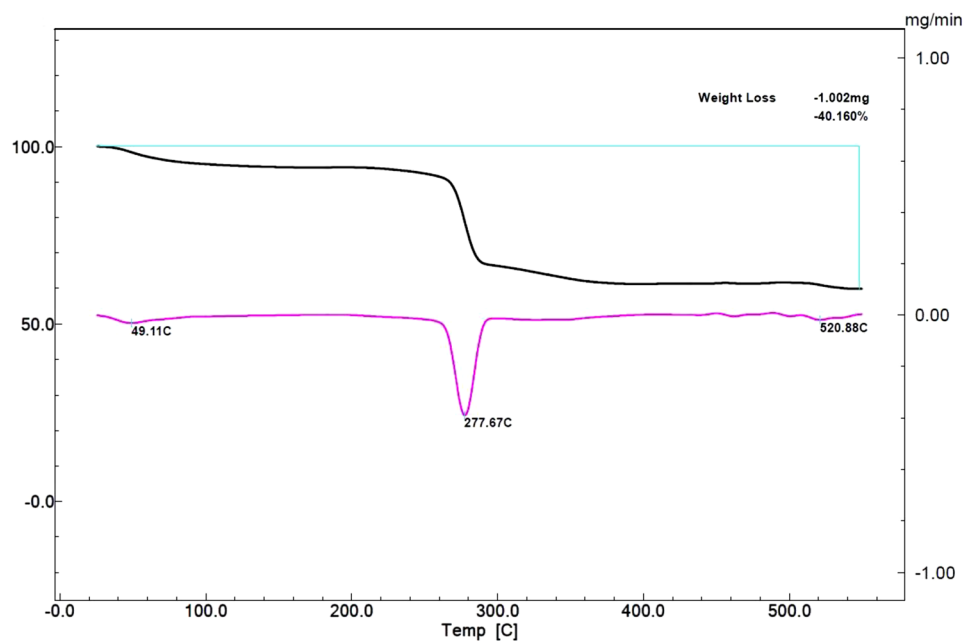
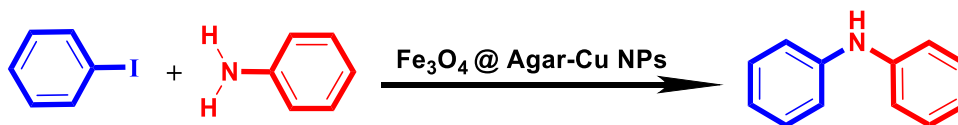
As it is presented in Table 3, the comparison of this catalyst with some recently published catalysts has been performed. Various conditions have been applied, but the use of green and nontoxic reaction conditions has not been reported. Employing reachable and no harmful materials, achieving high yields of product, and mild reaction condition is the art of this study.

In order to find the validity of the catalyst on a large scale reaction, the model reaction was also evaluated and the satisfying yield was observed (yield =  $82\%$ ). The used reaction conditions were Aniline (20 mmol, 1.86 g), Iodobenzene (20 mmol, 4.08 g),  $\text{K}_2\text{CO}_3$  (20 mmol, 2.76 g),  $\text{Fe}_3\text{O}_4$ @Agar-CuNPs (200 mg) and water (10 ml).

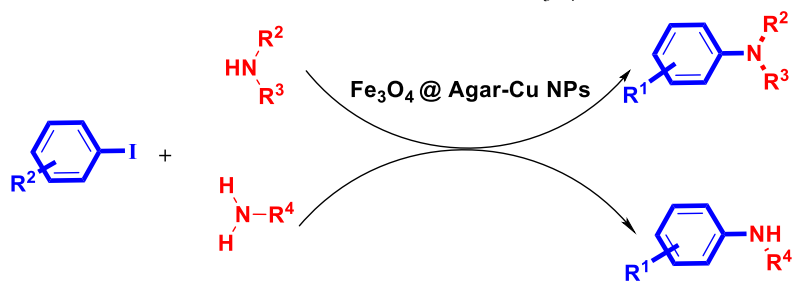
To check the catalyst's reusability on the model reaction, the nanocatalyst was removed easily from the mixture after the termination of the reaction, washed with ethanol and deionized water successively, and dried in vacuum oven. Soon afterward, the catalyst applied directly for the next run. However, this catalyst was reused for five times and shown good efficiency in the reaction process by the use of ICP analyses without significant leaching of Cu NPs (Fig. 9; Table 4).

The possible mechanism of C-N cross-coupling is the same as C-C cross-coupling reactions [22]. Including oxidative addition of the arylhalide to a  $\text{Cu}^0$  nanoparticle, the addition of the amine to the oxidative addition complex, deprotonation



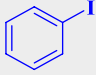
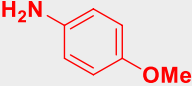
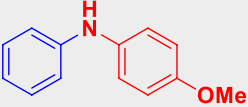
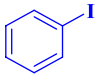
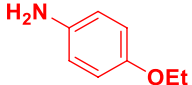
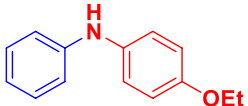
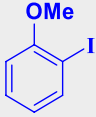
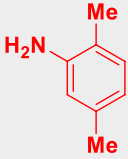
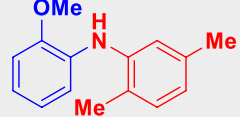
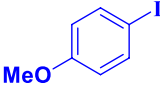
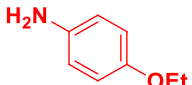
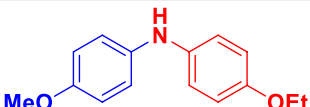
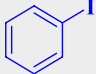
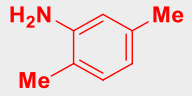
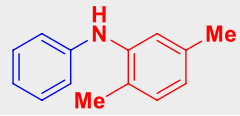
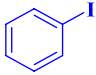
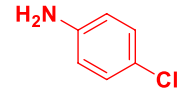
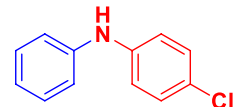
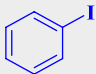
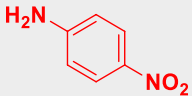
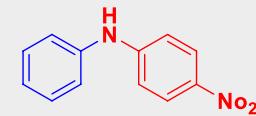
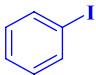
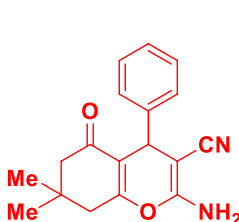
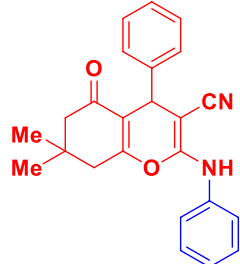
**Fig. 8** Thermogravimetric analysis of Fe<sub>3</sub>O<sub>4</sub>@Agar-Cu NPs**Table 1** The Optimization of the model reaction conditions

Entry	Catalyst (mol%)	Temperature (°C)	Solvent	Time (h)	Yield (%)
1	0	110	DMF	10	Trace
2	3	80	DMF	18	10
3	3	100	DMF	18	21
4	5	100	DMF	15	48
5	8	120	DMSO	16	70
6	8	100	H <sub>2</sub> O	12	68
7	8	80	H <sub>2</sub> O	15	55
8	10	120	DMSO	10	83
9	10	100	Toluene	12	80
10	10	100	DMF	12	94
11	10	100	H <sub>2</sub> O	12	96

**Table 2** C–N reaction cross-coupling derivatives of arylhalides and arylamines using  $\text{Fe}_3\text{O}_4@ \text{Agar-Cu NPs}$ 

Entry	Arylhalides	ArylAmines	Product	TON	TOF( $\text{h}^{-1}$ )	Yield (%)
1 <sup>a</sup>				9.4	0.78	94
2 <sup>a</sup>				8.8	0.73	88
3 <sup>a</sup>				9	0.75	90
4 <sup>a</sup>				9.3	0.77	93
5 <sup>a</sup>				9	0.75	90
6 <sup>b.1</sup>				9.6	0.80	96
6 <sup>b.2</sup>				9	0.75	90
7 <sup>b</sup>				9	0.75	90
8 <sup>b</sup>				8.5	0.70	85

Table 2 (continued)

9 <sup>b</sup>				8.3	0.69	83
10 <sup>b</sup>				8	0.66	80
11 <sup>b</sup>				8.2	0.68	82
12 <sup>b</sup>				8	0.66	80
13 <sup>b</sup>				8.9	0.74	89
14 <sup>b</sup>				9.1	0.75	91
15 <sup>b</sup>				9	0.75	90
16 <sup>b</sup>				8.8	0.73	88

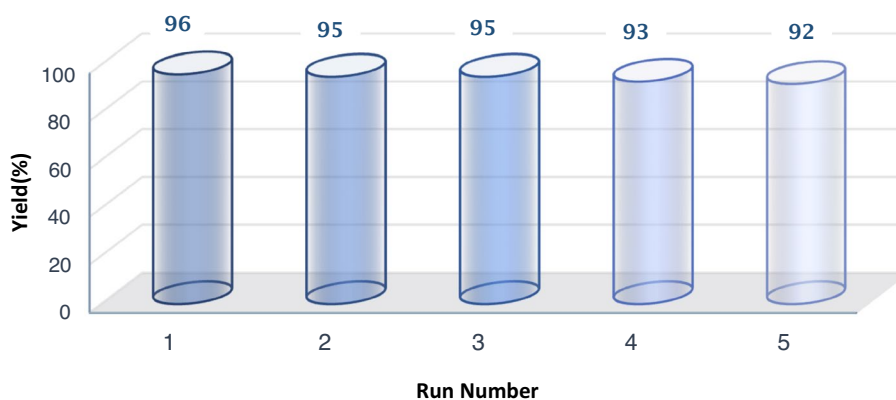
<sup>a</sup>Reaction conditions for secondary amines: H<sub>2</sub>O (4 ml), K<sub>2</sub>CO<sub>3</sub> (2 mmol), catalyst (10 mol%), temperature (100 °C), reaction time (12 h)

<sup>b</sup>Reaction conditions for primary conditions: H<sub>2</sub>O (0.5 ml), K<sub>2</sub>CO<sub>3</sub> (1 mmol), catalyst (10 mol%), temperature (100 °C), reaction time (12 h)

**Table 3** Comparison of catalytic activity of the Fe<sub>3</sub>O<sub>4</sub>@Agar-Cu NPs C–N cross-coupling of amines with aryl halides

Entry	Condition	Time (h)	Yield (%)	Ref
1	Fe <sub>3</sub> O <sub>4</sub> @PDA/Pd(II)–Cs <sub>2</sub> CO <sub>3</sub> –DMF at 100 °C	10	80	[34]
2	Pd(IPr*me)(acac)Cl–LiHMDS, 1,4-dioxane 110 °C	3	75–90	[58]
3	Toluene, NaOtBu, Pd/ligand 1:2, phosphonium salt: EtFluPCy <sub>2</sub> ·HBF <sub>4</sub> , 120 °C	12	48–95	[59]
4	Pd <sub>2</sub> (dba) <sub>3</sub> , XhantPhos, DBU, DMF, 100 °C	18	70	[60]
5	NHC-ligated Ni(I) Complexes, THF, 40 °C, <i>t</i> -BuONa	24	95	[36]
6	Cu(0)@Al <sub>2</sub> O <sub>3</sub> /SiO <sub>2</sub> NPs, K <sub>2</sub> CO <sub>3</sub> , DMF, N <sub>2</sub> , 150 °C	2–4	50–96	[61]
7	Fe <sub>3</sub> O <sub>4</sub> @Agar-Cu NPs–K <sub>2</sub> CO <sub>3</sub> , H <sub>2</sub> O, 100 °C	12	80–96	Current work



**Fig. 9** Reusability of the catalyst for the model reaction**Table 4** ICP analysis of Fe<sub>3</sub>O<sub>4</sub>@Agar–Cu NPs

	Cu	Fe
Conc 1	16.46 (%)	38.930 (%)
Conc 2	15.230	36.364 (%)
Conc MinRange	–	–
Conc Mean	15.846	37.647 (%)
Conc MaxRange	–	–
Reported	15.846	37.647

followed by reductive elimination of the species intermediate releases the desired product amines and complete the reaction cycles.

### 3 Experimental

#### 3.1 Preparation of Agar-Coated Magnetic Nanoparticles: Fe<sub>3</sub>O<sub>4</sub>@Agar NPs

Fe<sub>3</sub>O<sub>4</sub>@Agar magnetic nanoparticles were synthesized by dissolving a mixture of FeCl<sub>3</sub>·6H<sub>2</sub>O (9.2 mol, 2.46 g) and FeCl<sub>2</sub>·4H<sub>2</sub>O (4.6 mol, 0.91 g) in deionized water (150 ml) under vigorous stirring. Then, NH<sub>4</sub>OH solution (25% w/w, 10 ml) was added dropwise to the stirring mixture under the argon's atmosphere. Afterward, the solution of Agar (1.5 g) in water (50 ml) was added slowly to this mixture. The resulting solution is mechanically stirred for 5 h at 70 °C under the N<sub>2</sub> atmosphere. The resulting black material was separated using magnetic decantation and washed with deionized water (3 × 20 ml), and dried at 40 °C for 48 h.

#### 3.2 Synthesis of Copper Nanoparticles Coated Magnetic Agar: Fe<sub>3</sub>O<sub>4</sub>@Agar–Cu NPs

Fe<sub>3</sub>O<sub>4</sub>@Agar (0.8 g) was dispersed in deionized water (80 ml) in an ultrasonic bath for 15 min. Then, an aqueous

solution of CuCl<sub>2</sub> (50 g/l) is added dropwise over, for 15 min at room temperature. The mixture is mechanically stirred for the other 3 h. Subsequently, NaBH<sub>4</sub> (500 mg) is gently added to the mixture and stirred for 4 h. The color of the solution is changed from colorless to dark brown during the reaction. Eventually, Fe<sub>3</sub>O<sub>4</sub>@Agar–Cu NPs are separated by an external magnet, washed several times with water, and dried in a vacuum desiccator at room temperature.

#### 3.3 General Procedure for C–N Cross-Coupling Reactions

To a mixture of primary amine or secondary amine derivative (1 mmol) and the appropriate aryl iodide (1.1 mmol) in water (0.5 ml for primary amines and 4 ml for secondary amines) and K<sub>2</sub>CO<sub>3</sub> (1 mmol for primary amines and 2 mmol for secondary amines), Fe<sub>3</sub>O<sub>4</sub>@Agar–Cu NPs (10 mol%) was added, and the mixture is refluxed at 100 °C for 12 h. The progress of the reaction was monitored by TLC. After completing the reaction, the catalyst was separated using an external magnet, and the crude product is extracted from the aqueous phase by EtOAc. Finally, the pure products were isolated using column chromatography on silica gel using n-hexane/EtOAc as eluent.

### 4 Conclusion

In conclusion, we have demonstrated a noble, stable, versatile, and unique catalyst named Fe<sub>3</sub>O<sub>4</sub>@Agar–Cu NPs replaced for specific Ullmann Cross-Coupling catalyst reaction that usually used expensive and inaccessible Pd metal. Considering Agar as a pure and natural linker and also water as an eco-friendly solvent made this reaction undoubtedly a Green process. There is no harsh condition and surpass than the old method. More importantly, this catalyst effort both primary and secondary amines with significant yields that represent various derivatives.

**Supplementary Information** The online version contains supplementary material available at <https://doi.org/10.1007/s10904-021-02106-x>.

**Acknowledgements** The authors gratefully acknowledge the Research Council of Ferdowsi University of Mashhad (3/52357).

**Data availability** 7,7-dimethyl-5-oxo-4-phenyl-2-(phenylamino)-5,6,7,8-tetrahydro-4H-chromene-3-carbonitrile (Table 2, entry 16): white solid: mp 208–212 °C. <sup>1</sup>H NMR (300 MHz, CDCl<sub>3</sub>) δ (ppm): 1.21 (s, 6H, CH<sub>3</sub>), 1.80 (s, 1H, CH), 2.58 (s, 2H, CH<sub>2</sub>), 3.30 (s, 2H, CH<sub>2</sub>), 7.23–7.62 (m, 10H, Ar–H). <sup>13</sup>C NMR (75 MHz, CDCl<sub>3</sub>) δ (ppm): 195.1, 150.9, 131.2, 130.6, 129.0, 128.8, 128.5, 127.5, 119.4, 115.0, 58.3, 53.1, 43.6, 33.2, 30.9, 28.2.

## References

- E. Eidi, M.Z. Kassaei, P.T. Cummings, *Res. Chem. Intermed.* **44**, 5787 (2018)
- R.A. Sheldon, *Green Chem.* **7**, 267 (2005)
- Y. Shi, Z. Lyu, M. Zhao, R. Chen, Q.N. Nguyen, Y. Xia, *Chem. Rev.* **121**, 649 (2021)
- A. Maleki, Z. Hajizadeh, K. Valadi, *Green Chem. Lett. Rev.* **14**, 60 (2021)
- A. Maleki, *Ultrason. Sonochem.* **40**, 460 (2018)
- F. Schroeter, J. Soellner, T. Strassner, *Organometallics* **37**, 4267 (2018)
- M. Sarmah, M. Mondal, U. Bora, *ChemistrySelect* **2**, 5180 (2017)
- Y.H. Liu, H.C. Hu, Z.C. Ma, Y.F. Dong, C. Wang, Y.M. Pang, *Monatshfte Fur Chemie* **149**, 551 (2018)
- R. Eivazzadeh-Keihan, H.A. MoghimAliabadi, F. Radinekiyan, M. Sobhani, F. Khalili, A. Maleki, H. Madanchi, M. Mahdavi, A.E. Shalan, *RSC Adv.* **11**, 17914 (2021)
- N. Zohreh, S.H. Hosseini, M. Tavakolizadeh, C. Busuioic, R. Negrea, *J. Mol. Liq.* **266**, 393 (2018)
- A. Maleki, S. Azadegan, *J. Inorg. Organomet. Polym. Mater.* **27**, 714 (2017)
- M.M. Heravi, Z. Kheilkordi, V. Zadsirjan, M. Heydari, M. Malmir, *J. Organomet. Chem.* **861**, 17 (2018)
- H. Hammoud, M. Schmitt, E. Blaise, F. Bihel, J.J. Bourguignon, *J. Org. Chem.* **78**, 7930 (2013)
- P.A. Forero-Cortés, A.M. Haydl, *Org. Process Res. Dev.* **23**, 1478 (2019)
- H. Christensen, S. Kiil, K. Dam-Johansen, O. Nielsen, M.B. Sommer, *Org. Process Res. Dev.* **10**, 762 (2006)
- A.R. Hajipour, M. Check, Z. Khorsandi, *Appl. Organomet. Chem.* **31**, 1 (2017)
- M.S.S. Adam, F. Ullah, M.M. Makhlof, *J. Am. Ceram. Soc.* **103**, 4632 (2020)
- A.C. Flick, C.A. Leverett, H.X. Ding, E. McInturff, S.J. Fink, C.J. Helal, C.J. O'Donnell, *J. Med. Chem.* **62**, 7340 (2019)
- A. Maleki, *Tetrahedron* **68**, 7827 (2012)
- A. Maleki, *RSC Adv.* **4**, 64169 (2014)
- A. Maleki, *Tetrahedron Lett.* **54**, 2055 (2013)
- S.A. Mousavi Mashhadi, M.Z. Kassaei, E. Eidi, *Appl. Organomet. Chem.* **33**, 1 (2019)
- Z. Li, S. Ji, Y. Liu, X. Cao, S. Tian, Y. Chen, Z. Niu, Y. Li, *Chem. Rev.* **120**, 623 (2020)
- A. De Cattelle, A. Billen, W. Brullot, T. Verbiest, G. Koeckelberghs, *J. Organomet. Chem.* **899**, 120905 (2019)
- V.T. Trang, L.T. Tam, N. Van Quy, T.Q. Huy, N.T. Thuy, D.Q. Tri, N.D. Cuong, P.A. Tuan, H. Van Tuan, A.T. Le, V.N. Phan, *J. Electron. Mater.* **46**, 3381 (2017)
- Q. Zhao, C. Qian, X.Z. Chen, *Monatshfte Chem.* **144**, 1547 (2013)
- S. Bagheri, F. Pazoki, I. Radfar, A. Heydari, *Appl. Organomet. Chem.* **34**, 1 (2020)
- S.A. Mousavi-mashhadi, A. Shiri, *ChemistrySelect* **6**, 3941 (2021)
- A. Aranyos, D.W. Old, A. Kiyomori, J.P. Wolfe, J.P. Sadighi, S.L. Buchwald, *J. Am. Chem. Soc.* **121**, 4369 (1999)
- H. Christensen, S. Kiil, K. Dam-Johansen, O. Nielsen, *Org. Process Res. Dev.* **11**, 956 (2007)
- M. Keyhaniyan, A. Shiri, H. Eshghi, A. Khojastehnezhad, *New J. Chem.* **42**, 19433 (2018)
- A. Maleki, R. Taheri-Ledari, R. Ghalavand, R. Firouzi-Haji, *J. Phys. Chem. Solids* **136**, 109200 (2020)
- J.P. Wolfe, H. Tomori, J.P. Sadighi, J. Yin, S.L. Buchwald, *J. Org. Chem.* **65**, 1158 (2000)
- H. Veisi, P. Sarachegol, S. Hemmati, *Polyhedron* **156**, 64 (2018)
- R. Ayothiraman, S. Rangaswamy, P. Maity, E.M. Simmons, G.L. Beutner, J. Janey, D.S. Treitler, M.D. Eastgate, R. Vaidyanathan, *J. Org. Chem.* **82**, 7420 (2017)
- T. Inatomi, Y. Fukahori, Y. Yamada, R. Ishikawa, S. Kanegawa, Y. Koga, K. Matsubara, *Catal. Sci. Technol.* **9**, 1784 (2019)
- M. Esmaeilpour, J. Javidi, *J. Chin. Chem. Soc.* **62**, 614 (2015)
- V. Mishra, A. Arya, T.S. Chundawat, *Curr. Organocatal.* **7**, 23 (2019)
- F. Dai, Q. Gui, J. Liu, Z. Yang, X. Chen, R. Guo, Z. Tan, *Chem. Commun.* **49**, 4634 (2013)
- A.H. Dardir, P.R. Melvin, R.M. Davis, N. Hazari, M. MohadjerBeromi, *J. Org. Chem.* **83**, 469 (2018)
- V. Kandathil, B.D. Fahlman, B.S. Sasidhar, S.A. Patil, S.A. Patil, *New J. Chem.* **41**, 9531 (2017)
- L.J. Gooßen, B. Zimmermann, T. Knauber, *Angew. Chemie Int. Ed.* **47**, 7103 (2008)
- F. Bedos-Belval, A. Rouch, C. Vanucci-Bacqué, M. Baltas, *MedChemCommun* **3**, 1356 (2012)
- R. Fareghi-Alamdari, M.S. Saeedi, F. Panahi, *Appl. Organomet. Chem.* **31**, 1 (2017)
- C. Zhang, Y. Dai, Y. Wu, G. Lu, Z. Cao, J. Cheng, K. Wang, H. Yang, Y. Xia, X. Wen, W. Ma, C. Liu, Z. Wang, *Carbohydr. Polym.* **234**, 115882 (2020)
- E. Rafiee, A. Ataei, S. Nadri, M. Joshaghani, S. Eavani, *Inorganica Chim. Acta* **409**, 302 (2014)
- M.M. Mian, G. Liu, B. Yousaf, B. Fu, R. Ahmed, Q. Abbas, M.A.M. Munir, L. Ruijia, *J. Environ. Sci. (China)* **78**, 29 (2019)
- T. Baran, N. Yilmaz Baran, A. Menteş, *Int. J. Biol. Macromol.* **115**, 249 (2018)
- O.L. Kang, M. Ghani, O. Hassan, S. Rahmati, N. Ramli, *Food Hydrocoll.* **42**, 304 (2014)
- Y. Hou, X. Chen, Z. Chan, R. Zeng, *Process Biochem.* **50**, 1068 (2015)
- X.L. Chen, Y.P. Hou, M. Jin, R.Y. Zeng, H.T. Lin, *J. Agric. Food Chem.* **64**, 7251 (2016)
- S. Bahrami, F. Hassanzadeh-Afruzi, A. Maleki, *Appl. Organomet. Chem.* **34**, 1 (2020)
- Y.P. Yew, K. Shameli, M. Miyake, N.B.B. Ahmad Khairudin, S.E.B. Mohamad, T. Naiki, K.X. Lee, *Arab. J. Chem.* **13**, 2287 (2020)
- R. Armisen and F. Galatas, *Handb. Hydrocoll.* Second Ed. 82 (2009).

55. M. Keyhaniyan, A. Shiri, H. Eshghi, A. Khojastehnezhad, *Appl. Organomet. Chem.* **32**, 1 (2018)
56. Z. Ghadamyari, A. Shiri, A. Khojastehnezhad, S.M. Seyedi, *Appl. Organomet. Chem.* **33**, 1 (2019)
57. Z. Ghadamyari, A. Khojastehnezhad, S.M. Seyedi, A. Shiri, *ChemistrySelect* **4**, 10920 (2019)
58. X. Tian, J. Lin, S. Zou, J. Lv, Q. Huang, J. Zhu, S. Huang, Q. Wang, *J. Organomet. Chem.* **861**, 125 (2018)
59. C.A. Fleckenstein, H. Plenio, *Chem. - A Eur. J.* **13**, 2701 (2007)
60. S.K. Kashani, J.E. Jessiman, S.G. Newman, *Org. Process Res. Dev.* **24**, 1948 (2020)
61. P.L. Reddy, R. Arundhathi, D.S. Rawat, *RSC Adv.* **5**, 92121 (2015)

**Publisher's Note** Springer Nature remains neutral with regard to jurisdictional claims in published maps and institutional affiliations.